

# Monitoring of Bolted Joints with Electro-Mechanical Impedance Spectra and Acousto-Ultrasonics

---

A.-L. DREISBACH, P. KRAEMER and C.-P. FRITZEN

## ABSTRACT

Bolted connections are one of the most widely used types of joints in various fields of applications. Their functionality depends on the conservation of the preload in the bolt's shaft, which implies the need to monitor it. This paper addresses a monitoring procedure of the preload. Therefore, two measurement techniques for the preload are compared: On one hand, a technique, which is based on Electro-Mechanical Impedance spectra, on the other hand, a technique, which is based on Acousto-Ultrasonics. Electro-Mechanical Impedance spectra are measured with the help of the Electro-Mechanical Impedance method. This method is deployed in a relative high frequency range and the resulting spectra represent the transfer function between the local excitation of the structure and its response. In the applied Acousto-Ultrasonics procedure a burst excitation is introduced into the bolt on its head and the response is measured in pitch-catch mode at the face side of its shaft. As both techniques make use of so-called piezoelectric wafer active sensors, three different types of these transducers were used in this study and have been compared. For the experiments, three bolts having a size of  $M72 \times 380$  are equipped with the required transducers. Subsequently, they are tightened stepwise with a custom-built testing device for bolts. The several combinations of the measurement techniques and different types of piezoelectric wafer active sensors are then compared with focus on their sensitivity and variability. The most suitable combination in terms of preload monitoring is identified.

## INTRODUCTION

The operational safety of bolted joints depends mainly on the conservation of their preload. As preload losses can occur after a period of operation (i.e. due to self-loosening), the preload needs to be observed. In this work, two possible procedures for the measurement and monitoring of the preload in bolted joints are compared. The first one makes use of Electro-Mechanical Impedance (EMI) spectra and the second one is based on Acousto-Ultrasonics (AU). Both methods employ piezoelectric wafer ac-

TABLE I. Types of the used PWAS

PWAS-no.	Dimensions	Material	Shape
PWAS 1	20 mm x 1.96 mm ( $\varnothing$ x t)	PIC 155	Circular Disc
PWAS 2	20 mm x 0.25 mm ( $\varnothing$ x t)	PIC 151	Circular Disc
PWAS 3	50 mm x 30 mm x 0.8 mm (L x W x T)	PIC 255	Rectangular (DuraAct)

TABLE II. Positions of the used PWAS

Bolt no.	Bolt's head	Face side of bolt's shaft
Bolt 1	PWAS 1 (EMI, AU-Actuator)	PWAS 1 (AU-Sensor)
Bolt 2	PWAS 2 (EMI)	PWAS 2
Bolt 3	PWAS 3 (EMI, AU-Actuator)	PWAS 2 (AU-Sensor)

tive sensors (PWAS). Therefore, three types of PWAS are compared as well. For that comparison, the two measurement techniques are carried out with the different types of PWAS. For the evaluation of the combinations of measurement techniques and PWAS, one feature, which correlates with the preload, is taken into consideration for each technique, EMI and AU. This evaluation considers only the suitability of the technique and the used PWAS regarding the monitoring of the preload. The feature, which was selected in terms of the EMI approach, originates from previous investigations and is based on the changing trend of the susceptance. This changing trend occurs as a consequence of elastic deformations in the area of the bolt, where the PWAS is attached [1,2]. These deformations are caused by the applied preload. The feature which was selected regarding the AU-based procedure makes use of the phase shift of the ultrasonics wave propagation. This phase shift is caused by the applied mechanical stress [3]. The observation of this phase shift or time of arrival *TOA* can be used and related to the preload [4]. In this work, the *TOA* is estimated with the help of the Akaike's Information Criterion (*AIC*) picker. Both features are then examined with regard to their sensitivity and variability in order to assess the different combinations of the measurement techniques and the PWAS.

In the next section, the derivation and evaluation of the features will be described in more detail. Afterwards, the conducted experiments are presented as well as the results and discussion. In the last section, the conclusion and outlook are given.

## METHODS

In this work, two measurement techniques, which shall be applied for the monitoring of the preload using three different types of PWAS, are compared. Therefore two features, that correlate with the preload, one determined from each measurement technique (EMI and AU), have been used. The derivation of both features is based on physical effects, which occur due to changes of the applied preload. The feature which has been used in order to evaluate the EMI spectra is the trend of the susceptance and has been proposed in [1, 5]. It will be shortly introduced in the following lines: The PWAS used for the measurement of the EMI spectra is located at the head of the bolt, which deforms elastically due to the application of the preload [6]. In [7], it has been

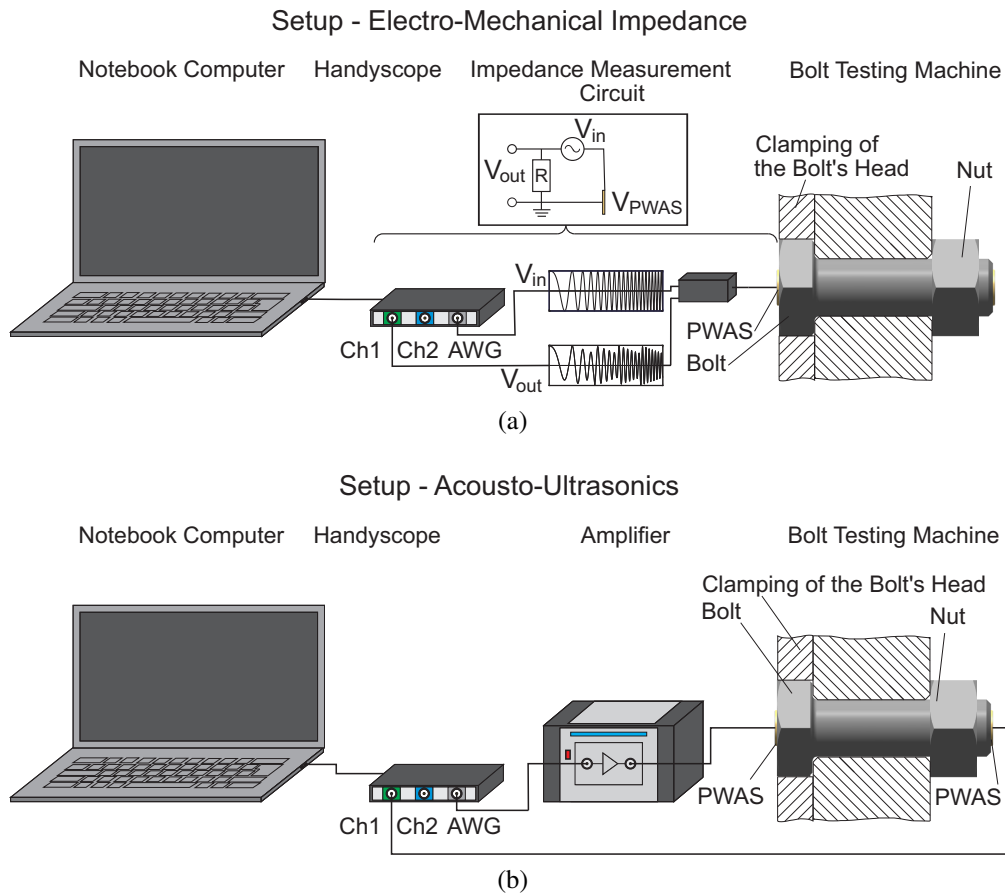


Figure 1. Experimental Setup and Measurement Devices: a) for EMI measurements, b) for Acousto-Ultrasonics measurements

found, that a mechanical deformation of the structure at the area, where the PWAS is attached, affects the properties of the PWAS additionally to its resonance behaviour. Therefore, a similar effect, which has been found in [7] can be observed at the PWAS at the bolt's head. Since the properties of the PWAS are affected and these properties are particularly well reflected in the susceptance, this quantity is observed for the preload monitoring. The susceptance can be found as the imaginary part of the reciprocal of the Electro-Mechanical Impedance. The effect of the changing preload on the susceptance is strongly visible in its changing trend. This trend is captured by the application of a robust regression algorithm [8]. The slope  $m_{Sus}$ , which results from this linear fit has been used to present the trend of the susceptance. Note, that the susceptance was observed in a narrow frequency range below the resonance frequency of the PWAS, where it shows almost linear behaviour. The deviations from the linear behaviour at the local resonances will be neglected by the robust fit algorithm.

For the evaluation of the AU measurements, the time of arrival (*TOA*) has been chosen as a feature, as a change of the *TOA* occurs due to the changing mechanical stress in the bolt's shaft between the actuating and sensing PWAS. The *TOA* can be correlated with the preload. There are two effects for the linear change in the *TOA*, which are both caused by the mechanical stress in the bolt's shaft [9]:

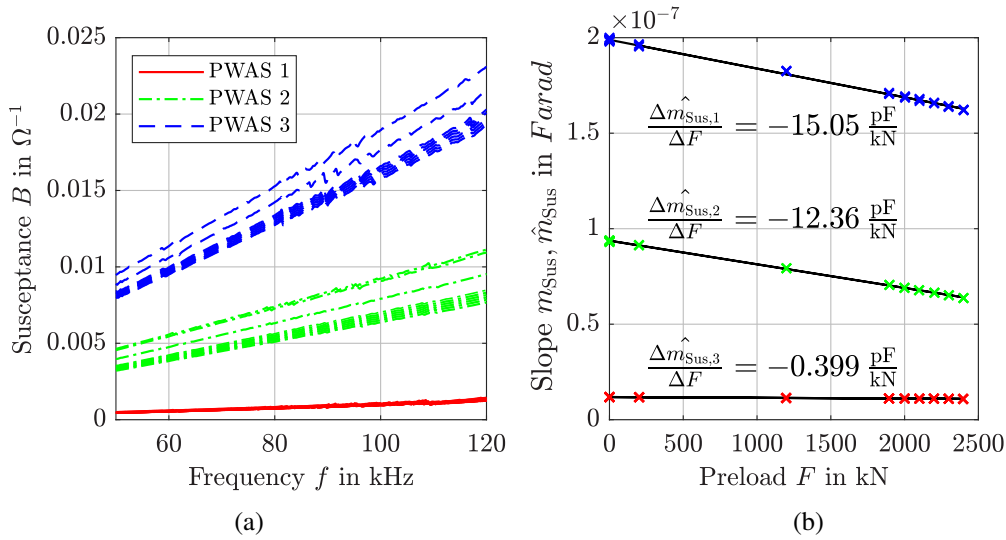


Figure 2. a) Effect of the preload on the susceptance spectra of the different types of PWAS b) Relation of  $m_{Sus}$  and the preload  $F$

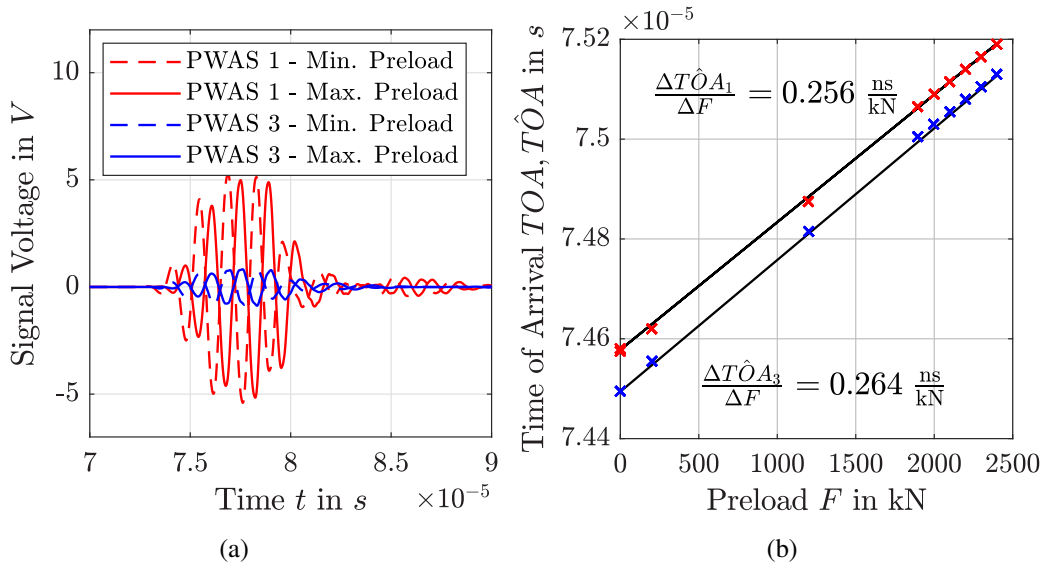


Figure 3. a) Influence of the preload on the TOA of Acousto-Ultrasonics measurement data b) Relation of TOA and the preload  $F$

1. The elongation of the bolt's shaft according to the Hooke's Law.
2. The changing wave speed: This phenomenon is known as acousto-elasticity. It considers the nonlinear-elastic relation between the mechanical stress and the distortion. This relation leads to an influence of the mechanical stress on the wave speed. The detailed derivation of the corresponding relations can be found in [3].

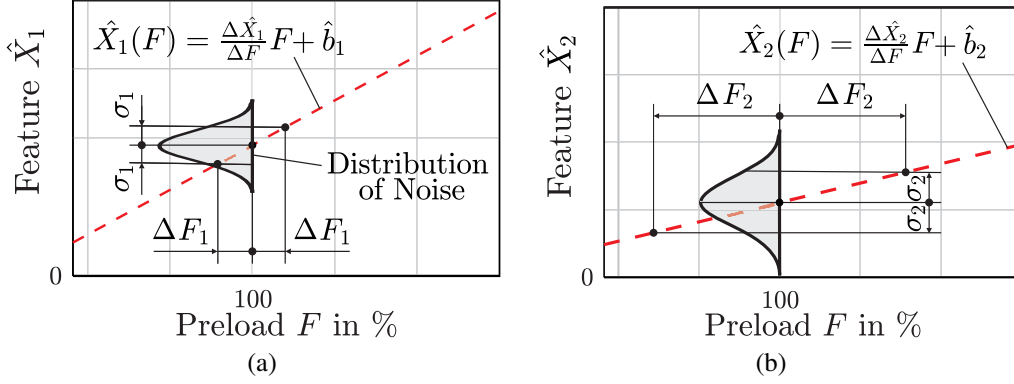


Figure 4. Effect of the sensitivity coefficient and the variability on  $\Delta F$  a) low variability and high sensitivity coefficient b) high variability and low sensitivity coefficient

The change in the *TOA* is captured with the help of the Akaike's Information Criterion (*AIC*) [10]. It was shown, that time series can be divided into two stationary segments, which can be modelled as two autoregressive processes, one corresponds to the noise and one to the signal. At the point where the *AIC* is minimized, the signal can be split into two time series. This point determines the onset point or *TOA* of the AU signal [11]. The *AIC* is presented in the following equation:

$$AIC(k) = t_k \log_{10} E\{(y_1^k)^2\} + (t_N - t_k - 1) \log_{10} E\{(y_{k+1}^N)^2\}. \quad (1)$$

Here, the time series  $y$  consists of  $N$  measurement points.  $E\{y^2\}$  corresponds to the sample variance and  $t_N$  is the sample time at the last measurement point  $N$ .  $t_k$  is the  $k$ -th point in time, where the time series is split into two parts:  $y_1^k$  reaching from the first to the  $k$ -th point and  $y_{k+1}^N$  reaching from the  $(k+1)$ -th point to the end of the time series.  $t_k$ , where the *AIC* is minimum is used to represent the *TOA*.

## EXPERIMENTS

In order to compare the EMI and AU measurement techniques, the experiments have been carried out on bolts having a size of M72 x 380 and the strength class of 10.9 according to DIN 14399-4 [12]. Three different types of PWAS have been installed on the head and the face side of the bolt's end. These types and their position can be found in the Tables I and II. In total three bolts have been investigated, which were tightened with a custom-built testing machine. The preload was applied stepwise starting at 0 kN until a maximum of 2 400 kN at room temperature. Special attention was paid to the higher range of preload, as this is the interesting range regarding preload loss detection. In DIN 25201-4 [13] a bolted connection is considered as non-functional at a loss of 20%. In this investigation this corresponds to a preload loss of 480 kN or a preload of 1 920 kN, respectively. Consequently, the range from 1 900 kN to 2 400 kN has been divided into smaller steps of 100 kN. At every preload stage, the EMI measurements have been carried out. The frequency range of the excitation signal has been set from 50 kHz to 120 kHz. Afterwards, the same tightening procedure has been repeated and the AU

measurements have been conducted. For the actuation, a Hanning windowed 5-cycle sine wave signal with a center frequency of 700 kHz has been used. Both measurement techniques have been carried out with a TiePie Engineering Handyscope HS5-540XMS and have been repeated ten times. For the EMI measurements, the same device has been used in order to build the circuit according to [14] and to measure the equivalent EMI spectrum with the help of an Ohmic resistor  $R$  as presented in Figure 1a. The EMI spectra are calculated from the excitation voltage at the PWAS  $V_{\text{PWAS}}$  as well as the current  $I$  in the frequency domain, which represents the response to the excitation. For the AU measurements, the excitation signal needed to be amplified in order to receive adequate amplitudes at the sensing PWAS. The measurement equipment for the AU measurements is shown in Figure 1b. Furthermore, in the case of both measurement techniques, 100 measurements have been carried out in order to investigate the variability of the data.

## RESULTS AND DISCUSSION

In this section, the results of the computed features are compared in order to propose a suitable combination of a measurement technique and a PWAS for a monitoring strategy of the preload. At the end, suggestions for the application of the investigated approaches are made. A selection of the EMI and AU measurement data are presented in the Figures 2a and 3a. In order to determine the sensitivity of  $m_{\text{Sus}}$  and the  $TOA$ , the two features have been plotted against the preload, which is shown in the Figures 2b and 3b. Their relation can be linearly approximated. The slopes  $\frac{\Delta \hat{m}_{\text{Sus}}}{\Delta F}$  or  $\frac{\Delta T\hat{O}A}{\Delta F}$  of that approximated relation can be interpreted as the sensitivity of the change in the feature to a change in the preload  $F$ . The greater the sensitivity, the better the preload can be resolved. The description of the sensitivity is comparable to the sensitivity coefficient described in [15]. Regarding the EMI-data, PWAS 3 shows the highest sensitivity with  $\frac{\Delta \hat{m}_{\text{Sus},3}}{\Delta F} = -15.05 \frac{\text{pF}}{\text{kN}}$  and PWAS 1 the lowest with  $\frac{\Delta \hat{m}_{\text{Sus},1}}{\Delta F} = -0.399 \frac{\text{pF}}{\text{kN}}$ . The sensitivities of the AU-data recorded by PWAS 1 and PWAS 3 are similar with  $\frac{\Delta T\hat{O}A_1}{\Delta F} = 0.256 \frac{\text{ns}}{\text{kN}}$  and  $\frac{\Delta T\hat{O}A_3}{\Delta F} = 0.264 \frac{\text{ns}}{\text{kN}}$ . The variability of the data caused by the measurement noise is described by the standard deviation  $\sigma$  as shown in Figure 4a. With the help of the sensitivity coefficient  $\frac{\Delta \hat{x}_1}{\Delta F}$ , this standard deviation is translated to a corresponding change of the preload  $\Delta F$ . This can be interpreted as follows: When the determined feature deviates from the linear relation by  $\pm\sigma$  due to the variability of the data, this leads to a deviation of  $\pm\Delta F$  in the preload. A good outcome for a measurement technique would be small deviations  $\Delta F$ . This would occur, if the procedure exhibits a high sensitivity coefficient and a low standard deviation as presented in Figure 4a. Because of the low variability, the deviations  $\Delta F_1$  from  $F$  are also low. The worst outcome would be a relatively small sensitivity coefficient and a high standard deviation as presented in Figure 4b. This would lead to high variations of  $\Delta F_2$  from  $F$  caused by the noise.

The results of the investigated sensitivity and variability are presented in Table III.  $\Delta F$  is expressed in % as percentage of the maximum preload 2 400 kN. Regarding the EMI-based data, PWAS 2 performs the best as a change of 0.42 % in preload corresponds to the standard deviation  $\sigma_{m_{\text{Sus},2}}$ . PWAS 1 performs the worst. With regard to the AU-based data, the measurements of PWAS 2 are not shown because this PWAS produced too small amplitudes, which made it impossible to estimate the  $TOA$  with the strategy

TABLE III. Variability and sensitivity of the two different strategies and the three different piezoelectric transducers

Strategy Bolt	EMI			AU		
	$\frac{\Delta \hat{m}_{\text{Sus}}}{\Delta F}$ [ $\frac{\text{pF}}{\text{kN}}$ ]	$\hat{\sigma}_{m_{\text{Sus}}}$ [pF]	$\Delta F$ [%]	$\frac{\Delta \hat{t}_{\text{OA}}}{\Delta F}$ [ $\frac{\text{ns}}{\text{kN}}$ ]	$\hat{\sigma}_{\text{TOA}}$ [ns]	$\Delta F$ [%]
Bolt 1	-0.40	41.88	4.38	0.256	2.26	0.37
Bolt 2	-12.36	125.17	0.42	—	—	—
Bolt 3	-15.05	458.32	1.27	0.264	2.36	0.41

presented here. The results of PWAS 1 and PWAS 3 with  $\Delta F = 0.37\%$  and  $\Delta F = 0.41\%$ , respectively, are similar, whereby PWAS 1 is slightly better. When Figure 3a is considered, the amplitude of PWAS 1 is significantly larger than the amplitude of PWAS 3, but with regard to the preload monitoring, this does not seem to have a large influence on the outcome. If the AU-based approach will be applied for the preload monitoring and an additional task at the same time, for example crack detection in the bolt's shaft, it might be better to choose the type PWAS 1, as due to the high amplitude there will be a good signal to noise ratio even after the elastic waves have interacted with a crack. If a combined procedure consisting of EMI and AU measurements shall be applied for preload monitoring, PWAS 3 would be the best choice, because its performance is quite the same for AU and with respect to the EMI-based data the 1.27% are still far away from 20% preload loss, which has to be detectable. Such a strategy might be more reliable as the informations of two measurement techniques (EMI and AU) are taken into account. A development of further approaches is necessary in order to compensate for temperature or other environmental effects, which was not considered in this study.

## CONCLUSION AND OUTLOOK

In this study, two procedures, one based on EMI and one on AU measurements, have been investigated in order to monitor the preload in bolted joints. The corresponding experiments have been carried out with three different types of PWAS. Two features, each for one of the measurement techniques, have been implemented, which show a linear dependence with the preload. These two features allow to estimate the variability using statistical confidence intervals for the respective method and PWAS. It turned out that one of the PWAS is best suited for EMI and one for AU measurements. In the case that both measurement techniques will be applied, the third type of PWAS can be used. As the preload was applied with the help of a testing machine for bolts, a next step should be to examine bolts that have experienced a loss of preload for example as a result of self-loosening.

## ACKNOWLEDGMENT

The research project IGF 20844 N / P1403 "Detektion von Vorspannkraftverlusten in Schrauben auf Basis elektromechanischer Impedanzspektren" from the Research Association for steel Application (FOSTA), Düsseldorf, was supported by the Federal Min-

istry of Economic Affairs and Climate Action through the German Federation of Industrial Research Associations (AiF) as part of the programme for promoting industrial cooperative research (IGF) on the basis of a decision by the German Bundestag. Furthermore, the authors would like to express their thanks to the company August Friedberg GmbH, which kindly provided the testing machine.

## REFERENCES

1. Dreisbach, A. L. and C. Fritzen. 2023. "A Novel Approach for Preload Monitoring in Bolted Connections Using Electro-Mechanical Impedance Spectra," in *European Workshop on Structural Health Monitoring*, Palermo, Italy.
2. Dreisbach, A. L. and C. Fritzen. 2022. "A novel approach for vibration-based preload-monitoring using electro-mechanical impedance spectra and probability of detection," in *Proceedings of ISMA2022 International Conference on Noise and Vibration Engineering USD2022 International Conference on Uncertainty in Structural Dynamics*, Leuven, Belgium.
3. Rose, J. L. 2004. *Ultrasonic waves in solid media*, Cambridge University Press.
4. Wang, T., G. Song, S. Liu, Y. Li, and H. Xiao. 2013. "Review of Bolted Connection Monitoring," *International Journal of Distributed Sensor Networks*, 9(12):871213.
5. Dreisbach, A.-L. and C.-P. Fritzen. 2021. "Monitoring von geschraubten Verbindungen mit elektromechanischen Impedanzspektren," in *3. VDI-Fachtagung Schwingungen 2021*, VDI Verlag GmbH, pp. 77–88.
6. Wang, T., B. Tan, G. Lu, B. Liu, and D. Yang. 2020. "Bolt Pretightening Force Measurement Based on Strain Distribution of Bolt Head Surface," *Journal of Aerospace Engineering*, 33(4):04020034.
7. Zhu, X. and F. Di Lanza Scalea. 2016. "Sensitivity to Axial Stress of Electro-Mechanical Impedance Measurements," *Experimental Mechanics*, 56(9):1599–1610.
8. Wetherill, G. B. 1986. *Regression Analysis with Applications*, Chapman and Hall, London.
9. Sun, Q., B. Yuan, X. Mu, and W. Sun. 2019. "Bolt preload measurement based on the acoustoelastic effect using smart piezoelectric bolt," 28(5):055005.
10. Klinkov, M. 2011. *Identification of unknown structural loads from dynamic measurements using robust observers*, Dr.-ing. dissertation, University of Siegen.
11. J. H. Kurz, C. U. Grosse, and H. W. Reinhardt. 2005. "Strategies for reliable automatic onset time picking of acoustic emissions and of ultrasound signals in concrete," *Ultrasonics* 43, 7:538–546.
12. DIN 14399-4. 2015, "High-strength structural bolting assemblies for preloading-Part 4: System HV - Hexagon bolt and nut assemblies," .
13. DIN 25201-4. 2021, "Design guide for railway vehicles and their components – Bolted joints: Part 4: Securing of bolted joints," .
14. D. M. Peairs, G. Park, and D. J. Inman. 2004. "Improving Accessibility of the Impedance-Based Structural Health Monitoring Method," *Journal of Intelligent Material Systems and Structures*, 15(2):129–139.
15. DIN 1319-1. 1995, "Fundamentals of metrology - Part 1: basic terminology," .